AFM Characterization of Emerging Photovoltaics

Introduction

As global energy needs continue to increase, sustainable technologies based on photovoltaic (PV) materials—those that directly convert light to electricity—offer a promising solution. Widespread commercialization of solar cell technology currently hinges on reducing cost,[1] which requires increasing power conversion efficiency, lowering manufacturing costs, and lengthening device lifetime. Success in each area depends on improved characterization techniques, especially in terms of higher spatial resolution. This need is driven by increasing use of materials with micro- and nanoscale features such as polycrystals in perovskite films, bulk heterojunction networks in organic semiconductors, and nanotextured light-trapping layers.

With its nanoscale spatial resolution, the atomic force microscope (AFM) provides complementary information to other imaging techniques[2] and tools that probe a whole device. Moreover, its ability to measure both structure and functional response enables deep insight into relations between structure, properties, processing, and performance (Figure 1). Here, we explore the power of today's AFMs for characterizing two emerging PV materials: perovskites and organic semiconductors. Although not discussed here, other materials such as inorganic semiconductors (e.g., Si, CdTe) and chalcopyrites (e.g., CIGSSe, $CuInSe_2$), and tandem systems with multiple absorbers can benefit from AFM characterization in analogous ways.

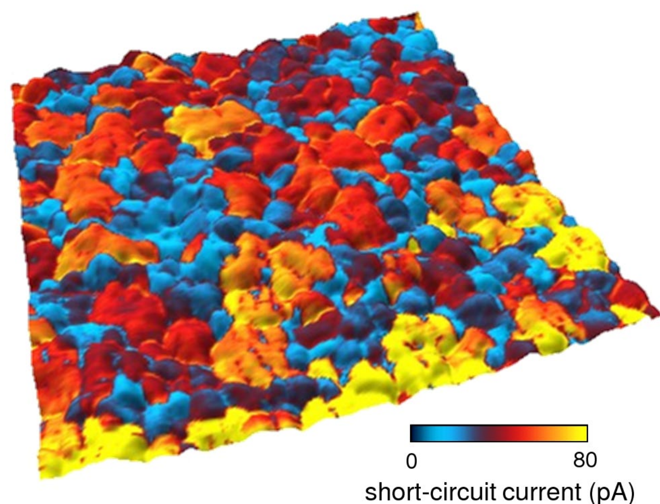

Figure 1: Visualizing nanoscale photoresponse in $MAPbI_3$
Solar-cell performance metrics such as short-circuit current I_{SC} are usually measured at the device scale, but characterization on the nanoscale can elucidate the crucial role of microstructure. The image shows short-circuit current I_{SC} overlaid on topography for a film of methylammonium lead triiodide ($CH_3NH_3PbI_3$ or $MAPbI_3$) under ~0.07 W/cm² illumination. It was obtained by first acquiring images of current with photoconductive AFM (pcAFM) at bias voltages ranging from 0 to +1 V. The images were then combined to form an I-V curve for each pixel location, from which values of I_{SC} were determined. Scan size 3 µm; acquired on the MFP-3D-BIO AFM. Adapted from Ref. 3.

Perovskites

Solar cell technology based on hybrid organic-inorganic perovskite materials is viewed with great excitement due to rapid gains in conversion efficiency, which reached >22% in just seven years.[1,4] Moreover, perovskite solar cells can be manufactured by relatively simple and inexpensive solution-processing techniques such as spin coating. Current research is focused on measuring fundamental properties and improving long-term stability. As discussed below, AFM techniques can supply important information to assist in both endeavors.[4]

Understanding Grain Structure

Evaluating the microstructure of perovskite films is beneficial for both fundamental and practical inquiries. For instance, it can elucidate the highly sensitive dependence of PV response on crystalline grain size and help address large-scale manufacturing issues such as how the perovskite crystallizes out of the precursor state.

To meet these needs, AFMs provide three-dimensional, quantitative maps of surface height or topography (Figure 2). Topography images reveal film attributes including coverage and uniformity, and allow rapid calculation of surface metrics such as roughness for quick comparison of different films. AFM topography images are acquired in either tapping or contact mode and typically resolve vertical features below a nanometer. In fact, some current-generation AFMs can achieve vertical resolution down to a few tens of picometers, enabling lattice-scale imaging of crystals and molecules. Newer AFMs also feature numerous automated routines that reduce experimental setup time and streamline data acquisition.

When perovskites are exposed to ambient conditions, irreversible changes in microstructure and other properties may occur due to oxidation or other chemical reactions. Such degradation can be prevented by performing AFM experiments in a purified, inert-gas environment using specialized measurement cells. These cells can also provide humidity control of ambient or inert gases. Even more stringent environmental control can be achieved by placing the entire AFM in a glovebox for complete atmospheric isolation (see Figure 5 and sidebar on page 8).

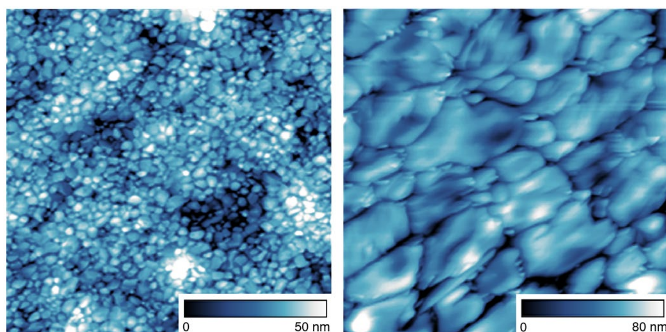

Figure 2: Altering grain structure
Solution-processing techniques can yield dense perovskite films with uniform surface coverage. However, these films are typically very fine grained, leading to increased grain-boundary losses and hence reduced photoconversion efficiencies. In this work, a guanidinium thiocyanate (GUTS) precursor treatment was developed to increase grain size. These topography images for (left) an untreated $MAPbI_3$ film and (right) a film post-treated with GUTS/isopropanol solution (4 mg/ml, GUTS-4) show that treatment increased the average grain size from nanometers to micrometers. In addition, the power conversion efficiency of solar cells prepared with GUTS-4-treated films increased by ~2% over that of cells with untreated films. Scan size 5 µm. Adapted from Ref. 5.

Measuring Electrical and Functional Response

Of course, many PV mechanisms require photoelectrical data to fully understand, and the polycrystalline structure of perovskite films impels measurement on the micro- and nanoscale. The AFM's capabilities for high-resolution electrical mapping can help investigate processes such as charge transport, trapping, and recombination, and related behavior. These techniques are even more powerful when performed on an AFM with sample illumination capabilities (see sidebar on page 6).

Maps of local current are obtained with conductive AFM (CAFM), also called photoconductive AFM (pcAFM) when performed under illumination. In both cases, a conducting tip is used to sense the current flowing from the sample under an applied DC bias voltage. Local variations in photoconductivity, photo-induced changes in carrier mobility, and related behavior can be imaged by scanning in contact or in a fast-force-mapping approach (see sidebar on page 4). To avoid signal artifacts, the AFM detection laser can be deactivated during the pcAFM measurements. Varying parameters such as bias voltage, illumination intensity, wavelength, or polarization can provide further information.

CAFM and pcAFM can also be used to obtain current-voltage (I-V) curves with nanoscale resolution The tip is placed in contact at a user-defined position, and the bias voltage is ramped while the current is measured. The resulting I-V curves lend insight into charge generation and injection, contact resistance, and the effects of annealing or other process variables (Figure 3).

CAFM and pcAFM impose special demands on the AFM's capabilities. Measurements need high sensitivity and low noise despite the fact that currents can span six orders of magnitude (picoamperes to microamperes). In addition, experiments that quantify the tip-sample contact area require calibration of the cantilever spring constant to determine the applied force.

Electrostatic force microscopy (EFM) and Kelvin probe force microscopy (KPFM) are other modes to evaluate photoelectric response. Their nanoscale spatial resolution means they can examine behavior within a single grain, or even a grain boundary, as well as grain-to-grain variations. Both EFM and KPFM measurements operate in tapping mode and are considered to approximately represent open-circuit behavior.

EFM senses electric field variations due to long-range electrostatic force gradients and is thus useful for detecting capacitive changes created by surface charges or embedded conductors. It is often a convenient way to obtain qualitative contrast quickly and easily. To minimize crosstalk from topography variations, a dual-pass scanning approach to EFM can be implemented.

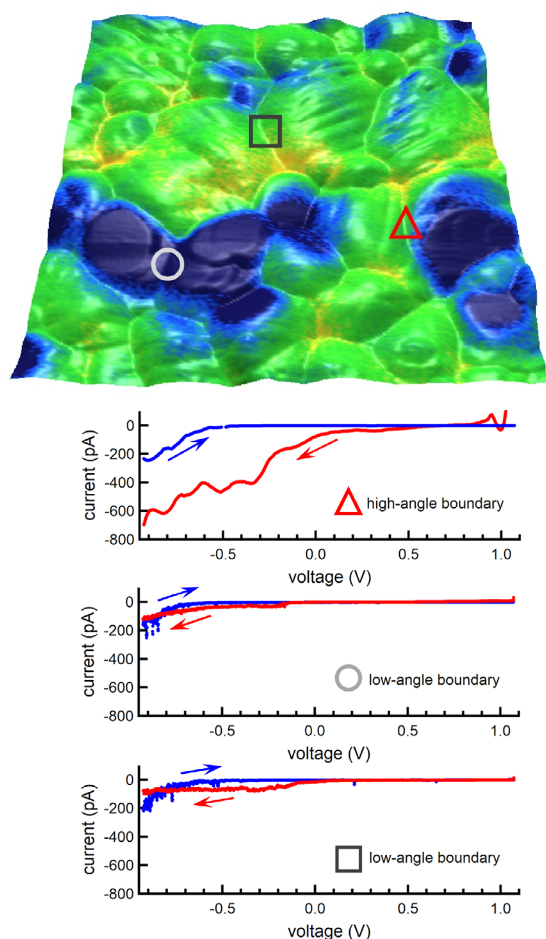

Figure 3: Investigating ion migration at grain boundaries
The mechanisms for many intriguing effects in perovskites such as current hysteresis and thermoelectricity are poorly understood. The image represents KPFM surface potential overlaid on topography for a polycrystalline $MAPbI_3$ film. Correlating surface potential with crystallographic orientation obtained by transmission electron microscopy (not shown) revealed that boundaries between grains with large surface potential differences (e.g., △) had higher angles than those with small potential differences (e.g., □ and ○). Local I-V curves acquired with CAFM showed strong dark-current hysteresis at the high-angle grain boundaries but very little hysteresis at low-angle boundaries. (Blue and red arrows indicate increasing and decreasing voltage, respectively.) The results indicated that grain-boundary migration was much faster than, and dominated over, migration within grains. Scan size 2 µm; acquired on the MFP-3D AFM. Adapted from Ref. 6.

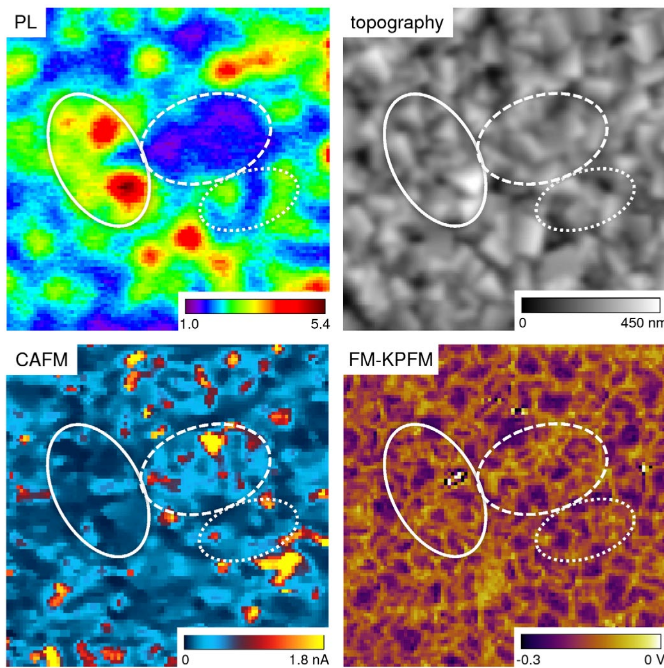

Figure 4: Correlating local optical and nanoelectrical properties
Understanding the origins of spatial heterogeneity in perovskite properties will help attain higher efficiency values. In this work, a methylammonium lead tribromide ($CH_3NH_3PbBr_3$ or $MAPbBr_3$) film was deposited on glass/indium tin oxide/poly(3,4-ethylenedioxythiophene) polystyrene (glass/ITO/PEDOT:PSS). Maps of local relative photoluminescence (PL) intensity were created by scanning a 488-nm laser beam across the bottom of a sample mounted on the AFM stage. Images of injected current acquired with CAFM (here, at +3.2 V bias) showed behavior anti-correlated with PL intensity. The dashed, dotted, and solid curves indicate regions with dim, intermediate, and bright PL response but high, intermediate, and low injected current, respectively, despite similar topography. Moreover, FM-KPFM surface potential images lacked any correlated behavior. Comparison to results for a $MAPbBr_3$ film on bare glass suggest that the heterogeneities arose from effects at the electrode-film interface, not within the film. Scan size 7 µm; acquired on the MFP-3D AFM. Adapted from Ref. 7.

In contrast, KPFM senses the contact potential difference between the tip and sample (Figures 3 and 4). One of KPFM's key benefits is the ability to quantitatively measure work function, an underlying cause of potential variations in many PV systems. Nanoscale imaging of work function with KPFM produces highly detailed information on band bending, dopant density, and photo-induced changes. KPFM is commonly performed in a dual-pass, amplitude-modulated (AM) approach similar to EFM, but it can also be operated in a single-pass, frequency-modulated (FM) mode. FM-KPFM often gives higher spatial resolution and contains additional information from the cantilever's higher-harmonic response.

Multimodal and correlated results can also yield a deeper understanding of PV materials. In this approach, complementary data are obtained with multiple AFM modes and/or other characterization tools such as scanning and transmission electron microscopy (SEM and TEM), photoluminescence (PL), and Raman spectroscopy. Examples are shown in Figure 3 (KPFM, CAFM, and TEM) and Figure 4 (CAFM, KPFM, and PL).

In addition, ferroelectric behavior in perovskites can impact performance in multiple ways. For instance, polarization fields can separate electron-hole pairs more efficiently, and charged domain walls can serve as additional conduction pathways. Ferroelectricity may also enable switching, whereby the photocurrent direction can be controlled by the bias voltage. However, attempts to leverage such behavior is hampered by limited understanding of relations between specific process conditions and the resulting ferroic properties. Improved characterization, especially on scales that match domain and grain sizes, is therefore crucial.

Piezoresponse force microscopy (PFM) is a powerful technique for characterizing ferroic properties. It is useful for nanoscale interrogation of both static and dynamic behavior such as domain structure, growth, and polarization reversal. By mapping electromechanical response as well as topography, PFM can provide deep insight into functional behavior and structure-property relations (Figure 5). In PFM measurements on thin films, the applied voltage must be high enough for good signal-to-noise ratio without causing polarization switching or even breakdown and damage. One solution involves operating near the cantilever's contact resonance frequency to achieve higher sensitivity at lower drive voltage.

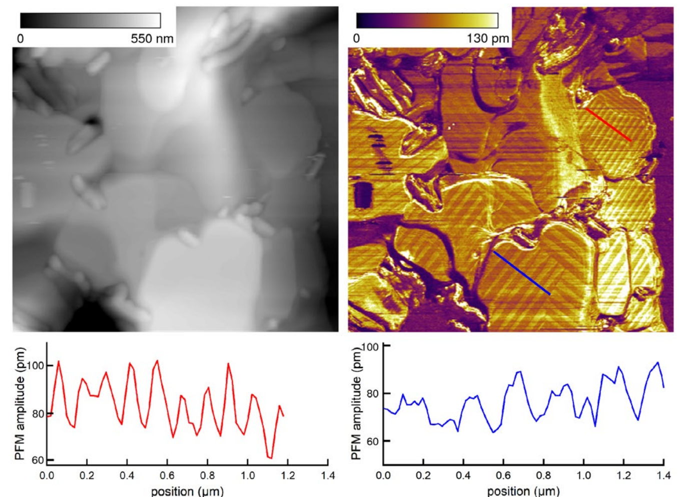

Figure 5: Detecting ferroelasticity
Topographic imaging (left) of a $MAPbI_3$ ($CH_3NH_3PbI_3$) film prepared by solvent annealing revealed micrometer-sized crystalline grains with a terraced structure. The corresponding image of vertical PFM amplitude (right) was acquired at 300 kHz (near resonance) with +2.5 V AC bias. Domains of regularly spaced stripes not present in the topography were observed, with 90° changes in orientation between adjacent domains. Sections across the color-coded lines in the PFM image show that the stripe periodicity varied and ranged from approximately 100 to 350 nm. The results suggest the film was ferroelastic, with a domain structure highly dependent on film texture and thus the specific preparation route. Scan size 7 µm. Acquired on the MFP-3D AFM in a glovebox with nitrogen. Adapted from Ref. 8.

Functional Imaging with Asylum AFMs

- The ORCA module ensures current measurements with high sensitivity over a wide dynamic range on MFP-3D and Cypher family AFMs. A low-noise transimpedance amplifier integrated into the cantilever holder operates from ~1 pA to 20 nA with a variety of gain options available. With the Dual Gain ORCA option, two separate amplifiers allow high-resolution measurements over an even wider current range (~1 pA to 10 µA).
- Eclipse Mode improves photocurrent measurements and reduces photo-induced artifacts on all Asylum AFMs using a dual-pass approach. In the first scan pass, topography is acquired in contact mode. In the second pass the AFM's detection laser is turned off, and pcAFM measurements are performed at the same height.
- Precise knowledge of absolute tip-sample contact forces is simpler with GetReal. Provided on all Asylum AFMs, this software automatically calibrates the cantilever spring constant and deflection sensitivity with a single click, without ever touching the sample.
- Fast Current Mapping Mode on Cypher family and MFP-3D Infinity AFMs offers powerful capabilities for current imaging, especially on soft or delicate materials. Current and force curve arrays are acquired simultaneously; at pixel rates up to 300 Hz (MFP-3D Infinity) or 1 kHz (Cypher family), 256×256-pixel images can be acquired in under 10 min.
- All Asylum Research AFMs include software for high-sensitivity, resonance-enhanced PFM measurements with Dual AC Resonance Tracking (DART) mode or the Band Excitation option. Asylum Research also offers high-voltage PFM (up to ±220 V for MFP-3D Origin+ AFM and ±150 V for MFP-3D Infinity and Cypher family AFMs).

Learn more

The Asylum website includes pages that describe the use of AFM for common research applications. These pages include relevant application notes, webinars, and selected publications. Please see these related pages:

- "AFM for Solar, Photovoltaics and Thermoelectrics Research" – http://AFM.oxinst.com/Solar
- "AFM Tools for Nanoscale Electrical Characterization" – http://AFM.oxinst.com/Nanoelectrical
- "AFM Tools for Piezoelectrics and Ferroelectrics Research" – http://AFM.oxinst.com/PFM

Engineering Interfacial Layers

The simplest solar cell geometry contains only a perovskite absorber layer sandwiched between two electrodes. However, designs often include additional layers to improve performance. AFM is valuable for characterizing these layers individually or in combination. Devices can be examined in plan view with the conducting AFM tip serving as the top contact or in cross section to examine behavior across and at interfaces.

Imaging nanoscale topography of interfacial layers gives information on surface roughness, which affects layer-to-layer adhesion, and reveals morphological features such as phase segregation and dispersion of organic films. Electrical modes such as CAFM and pcAFM are also useful, for instance to assess conduction uniformity or identify areas of charge trapping or recombination. KPFM characterization is particularly beneficial for its sensitivity to surface contact potential and work function. Because interfacial layers are often designed to create a more favorable route for carriers away from the absorber and toward an electrode, they must be chosen to improve the alignment of energy levels at each interface. KPFM can supply helpful feedback for this purpose by imaging spatial variations in band bending and work function (Figure 6).

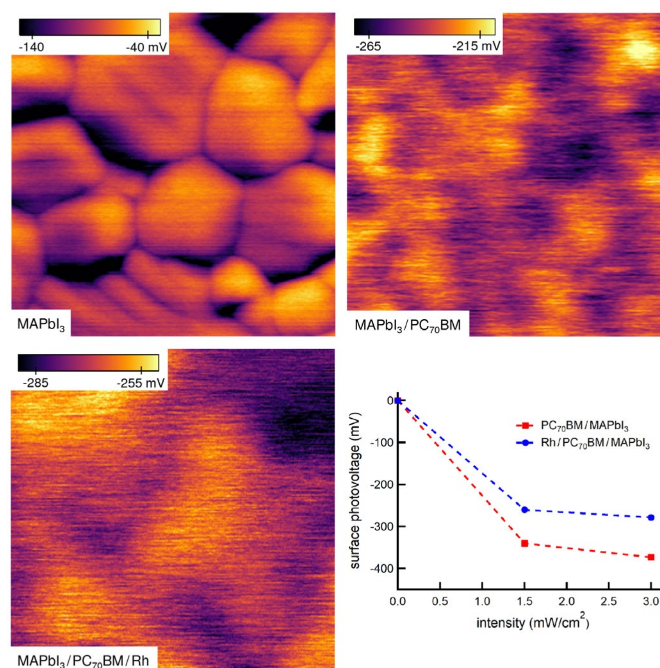

Figure 6: Improving stability with interlayers
Effective use of electron transport layers (ETLs) requires better control of their properties. These maps of surface potential were acquired on a $MAPbI_3$ ($CH_3NH_3PbI_3$) film on NiO_x before and after addition of phenyl-C_{71}-butyric acid methyl ester ($PC_{70}BM$) and rhodamine 101 (Rh) layers. The Rh layer significantly reduced spatial variations in potential by passivating defects at the perovskite grain boundaries. The graph of induced surface photovoltage (i.e., difference in surface potential from light to dark) shows the additional layers decreased surface potential, reducing band bending at the ETL/cathode interface. The results helped explain measurements of increased efficiency and stability for devices with Rh layers. Scan size 1 µm; acquired on the MFP-3D AFM in dual-pass KPFM mode. Adapted from Ref. 9.

Organic Semiconductors

Organic solar cells based on polymers and small organic molecules are also highly promising for next-generation PV technology. They use widely available, relatively eco-friendly materials and can be produced by simple, inexpensive techniques such as solution processing or vapor deposition. Because commercially-viable power conversion efficiencies (>10%) have already been achieved, increasing cell lifetime from years to decades is now considered the key hurdle to commercialization.[10] Critical to this effort is understanding how performance degrades due to light, heat, and other environmental factors. As described below, AFM measurements of local structure and properties can clarify these issues.[11]

Mapping BHJ Morphology

Organic solar cells typically use a bulk heterojunction (BHJ) photoabsorber containing a self-assembled, nanostructured network of donor and acceptor materials. Efficiency depends strongly on the network's specific phase segregation and connectivity, but predicting the structure formed by a given processing route remains challenging. In addition, morphology can change with time by various aging mechanisms. Characterizing the micro- and nanoscale morphology of BHJ films is therefore essential. Electron microscopy is a widely used option, but achieving sufficient image contrast often incurs sample damage.

AFM topographic imaging can reveal the size and dispersion of BHJ components and explore the effects of process variables such as solvent evaporation rate and annealing (Figure 7). Topographic imaging on organic materials is typically performed in tapping mode, which applies extremely gentle lateral and vertical tip-sample forces. Lower forces not only minimize sample damage but also achieve higher spatial resolution due to the smaller tip-sample contact area. Forces as low as sub-piconewtons can be resolved and controlled if very small cantilevers on newer, fast-scanning AFMs are used, an important consideration for delicate, easily deformed polymers.

BHJ morphology can also be characterized with AFM modes that sense mechanical properties. For example, phase imaging in tapping mode often gives contrast between blend components and resolves fine structural details. Elastic modulus maps obtained by force curve techniques can also reveal phase separation and dispersion (Figure 8). Other nanomechanical modes allow rapid, qualitative imaging as well as quantitative mapping of elastic and viscous response. In particular, newer bimodal tapping techniques such as AM-FM mode enable fast mapping with high spatial resolution.[14]

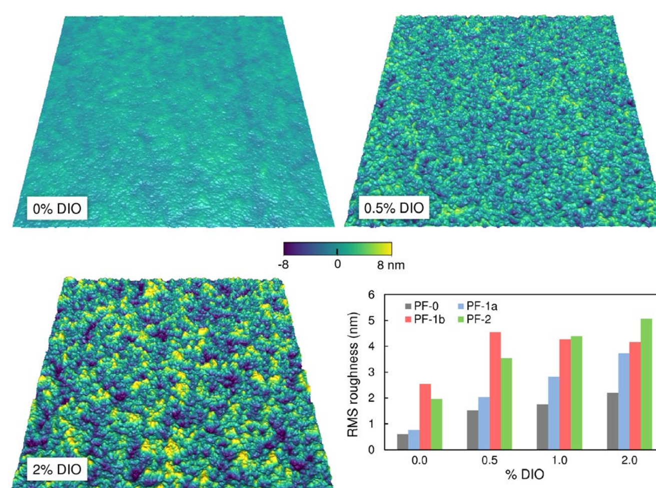

Figure 7: Tuning performance via fluorination
Substituting fluorine for hydrogen in the conjugated polymer backbone can enhance efficiency and durability. Here, systematic studies of this effect were performed on four narrow-band-gap polymers: PF-0 without fluorine, PF-1a and PF-1b with intermediate fluorine and different regioselectivity, and PF-2 with the most fluorine (see Ref. 12). Solution-processed films of polymer/$PC_{70}BM$ blends were created with varying amounts of the solvent additive DIO. These topography images for the PF-1a blend indicate that low amounts of DIO increased phase separation and thus improved power conversion efficiency, but higher amounts yielded sub-optimum morphology. The graph reveals that root-mean-squared roughness generally increased with fluorine content in all four blends, likely due to enhanced aggregation. Scan size 5 µm; acquired on the MFP-3D AFM in tapping mode. Adapted from Ref. 12.

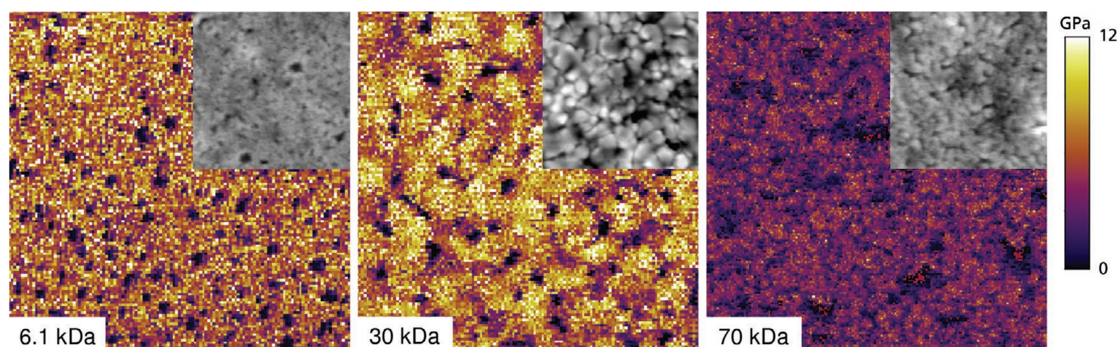

Figure 8: Evaluating molecular weight effects – Films were created containing blends of diketo-pyrrolopyrrole-thienothiophene polymer (PDPP4T-TT) and phenyl-C_{61}-butyric acid methyl ester (PCBM) with varying polymer chain number average molecular weights. Maps of Young's modulus acquired with force curve techniques allowed the separate BHJ phases to be identified, with lower and higher modulus values corresponding to PDPP4T-TT and PCBM, respectively. (Insets show the corresponding tapping-mode topography.) Large PCBM domains observed for the film with intermediate molecular weight indicated a PCBM-rich surface created by vertical segregation during spin casting. The result could explain the unusually low values of series resistance measured on a transistor made with this film. In contrast, the phases appeared well intermixed in the other films, which yielded transistors with higher series resistance. Scan size 3 µm; acquired on the Cypher AFM. Adapted from Ref. 13.

Photovoltaics Option for MFP-3D Infinity AFM

The PV option for the MFP-3D Infinity AFM offers a flexible, turnkey platform for improved AFM characterization of photoactive materials and systems. By adding customizable, bottom-side sample illumination to the MFP-3D's already extensive capabilities, it enables high-resolution characterization with a wide range of AFM techniques and environmental control options. Features include:

- Fiber-coupled LED allows a maximum illumination of >1 sun with intensity control of 1% (see figure, right)
- External light sources such as Hg-Xe lamps are easily accommodated using commercially-available adapter plates
- Open design enables insertion of Ø1" components such as filters, polarizers, and apertures in the optical path
- Quick-release adapters let you switch between multiple light sources and fibers in seconds
- Full compatibility with all MFP-3D Infinity environmental accessories for heating, cooling, and humidity control

The Infinity PV's optical components are located inside the base beneath the sample stage, with a hinged door for easy access. The sample can be illuminated with the included LED illuminator or a user-provided light source. Light is focused onto the sample by a lens with adjustable focus, enabling a range of sample thicknesses. Insertion points allow the addition of filters, polarizers, and other components for additional experimental flexibility.

Learn More: http://AFM.oxinst.com/Infinity-PV

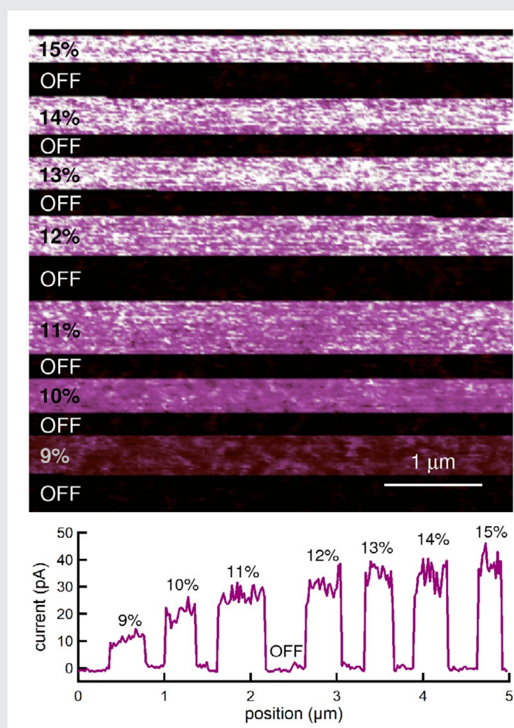

Here, the sample was a layer of poly(3-hexylthiophene) and phenyl-C_{61}-butyric acid methyl ester (P3HT:PCBM) bulk heterojunction annealed on an indium tin oxide (ITO) substrate. The sample was imaged at −1 V bias using the ORCA holder. During current imaging, the 530-nm illumination source was turned on and off while increasing the intensity in 1% increments (full power ~0.9 W/cm^2). The vertical section through the image reveals the dependence of measured current on intensity and demonstrates high sensitivity to small changes in intensity.

Imaging Nanoscale Photoresponse

Understanding charge injection, transport, trapping, and recombination remain key research priorities for organic semiconductors, to increase efficiency as well as reduce degradation in performance. AFM imaging of nanoscale photoresponse can yield valuable information about these mechanisms and pinpoint where in the BHJ each process occurs.

Imaging organic semiconductors with CAFM and pcAFM allows nanoscale visualization of photocurrent and charge transport networks in the donor-acceptor blend. These modes can therefore help determine the role that structural anisotropy, light intensity, or other parameters play in photoconversion (Figure 9).

However, the relatively soft and delicate nature of organic semiconductors makes them prone to damage by the lateral forces applied when using conventional contact-mode CAFM and pcAFM. Moreover, wear to both the sample and tip from contact-mode scanning can affect the measured current and complicate image interpretation. To avoid such issues, fast current mapping techniques have been developed in recent years. Fast current mapping moves the cantilever vertically in a continuous sinusoidal motion while it is also scanned laterally. Current is measured while acquiring a high-speed array of force curves. When performed under illumination, one may easily correlate topography and current data to elucidate local structure-property relations. These techniques also present many data analysis options, providing that complete curves of current and deflection versus time are saved.

EFM and KPFM also offer many benefits for electrical characterization of organic semiconductors. Mapping local variations in capacitance gradients with EFM or surface potential with KPFM can enable insights needed to improve device performance or long-term stability. The noncontact nature of these modes minimizes energy-barrier effects created by the tip's work function, so that measurements represent the system's open-circuit response.

EFM and KPFM images acquired by dual-pass scanning take a few minutes to acquire and thus are suitable for studying relatively slow processes. Faster processes, such as charge injection and carrier diffusion with timescales of milliseconds to seconds can be examined with other electrical modes. For example, FM-EFM and its offshoot, cantilever ringdown imaging, have been used to study photochemical degradation by imaging local variations in power dissipation and charge trapping.[15]

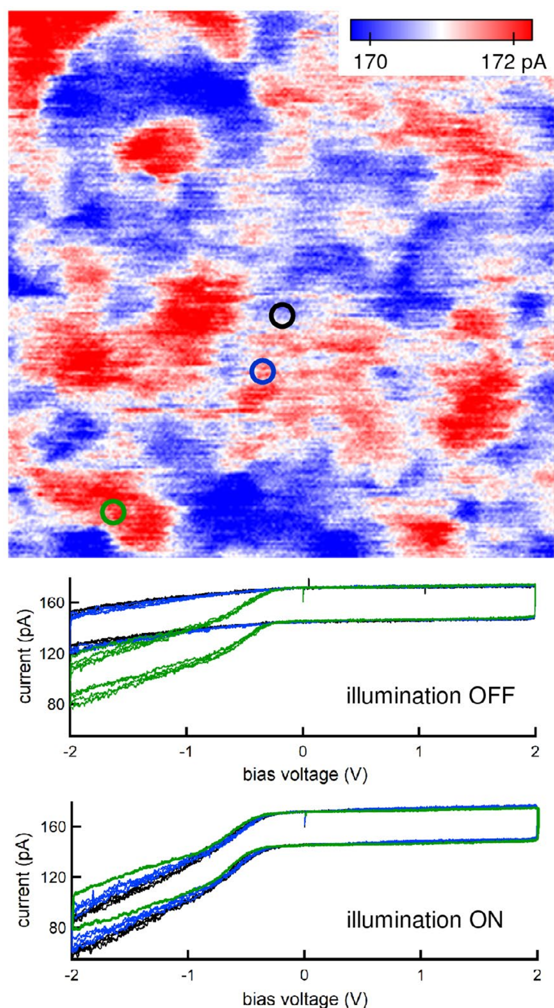

Figure 9: Exploring photocurrent heterogeneity in P3HT:PCBM
The pcAFM current image at +1 V bias reveals domains of higher and lower conductivity in a blend of poly(3-hexylthiophene) (P3HT) and PCBM. I-V curves for the color-coded positions in the image were acquired in the dark and while illuminated (~0.09 W/cm^2, 530 nm). In both cases, current increased with voltage below −0.3 V bias and then transitioned to much higher resistance at further positive bias. In some positions the amount of current flow depended on the illumination condition (e.g., black and blue circles), while it was always high in others (e.g., green circle). Hysteresis between the forward and reverse bias directions was also observed, indicative of sample capacitive charging. Scan size 1 µm. Acquired on the MFP-3D Infinity AFM with PV option and ORCA holder.

Additional techniques like time-resolved EFM and heterodyne KPFM have enabled dynamic studies of local charge carrier lifetime, photo-induced charging rates, and thermal annealing effects in both organic semiconductors and perovskites.[15,16] Although not standard on commercial AFMs, these techniques highlight the power of an open software platform. The open control architecture of all Asylum AFMs offers endless potential for modifying acquisition and analysis routines, for instance to synchronize measurements with illumination changes or combine commands into an automated batch procedure.

Optimizing Interlayers

Organic solar cells typically incorporate additional layers for functions such as extracting and receiving charge and controlling surface recombination. In designing layers to optimize performance, nanoscale information acquired with AFM techniques can prove essential. For instance, topographic imaging can evaluate changes in the BHJ morphology induced by the addition of interlayers, which can impact carrier recombination efficiency.[17] In addition, EFM and KPFM imaging across interfaces can provide information needed to design interlayers that better align electric fields and energy levels from the photoabsorber to the electrodes.

Layers can also improve long-term device stability, for instance by inverting geometries or even complete encapsulation. For AFM studies of stability and lifetime, environmental control can be desirable or even critical. It permits exposed devices to be surrounded by an inert gas and allows experiments to be performed under realistic or enhanced humidity (Figure 10). Temperature is another important aspect of AFM environmental control; it is usually achieved with specialized stages that give stable, precise temperatures up to several hundred degrees.

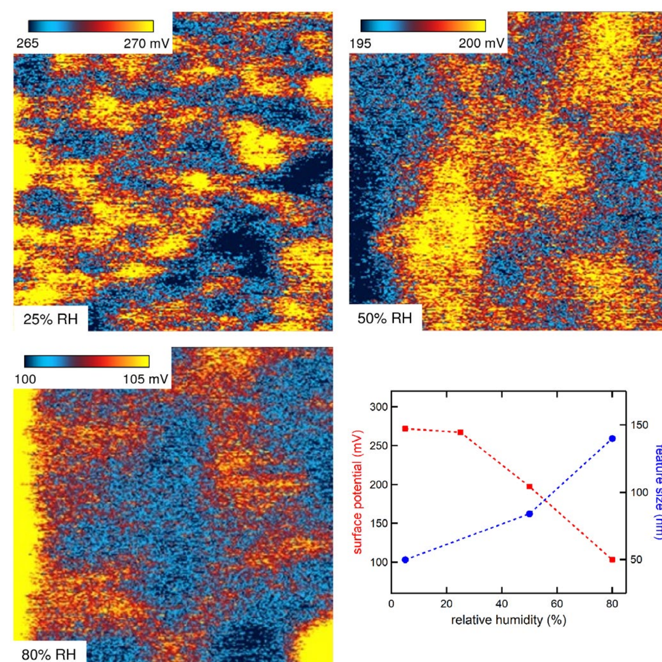

Figure 10: Characterizing humidity-dependent effects
P-type metal oxides could serve as effective hole extraction layers in organic solar cells, but the impact of environmental conditions on their electrical properties is not fully understood. In this work, KPFM imaging of a polycrystalline NiO_x film revealed nanoscale spatial variations in surface potential that depended on relative humidity (RH). The average value of surface potential decreased with increasing RH, while the average size of topographical features increased. This behavior is consistent with charge screening due to water adsorption on the film surface. The observed spatial irregularities in surface potential most likely arose from uneven chemisorption by exposed crystallites of different orientations. Scan size 1 µm; acquired on the Cypher AFM. Data courtesy of the Center for Nanophase Materials Sciences, Oak Ridge National Laboratory; adapted from Ref. 18.

Environmental Control for Oxygen- and Water-Sensitive PV Materials

- Many PV materials can be irreversibly compromised by surface chemical reactions with ambient oxygen or water vapor. To avoid sample degradation or simply reduce the water layer for more reliable electrical measurements, Turnkey Glovebox Solutions provide full environmental isolation on both the MFP-3D and Cypher family AFMs.
- Environmental isolation can also be achieved with the Closed Fluid Cell for MFP-3D AFMs and the Liquid Perfusion Cantilever Holder for Cypher ES AFMs. The sample and cantilever are mounted in these units inside an external glovebox, and the inlet ports are plugged. The entire sealed unit is then placed on the AFM for measurements without atmospheric exposure.

Conclusions

Photovoltaic technologies are already helping to meet the world's ever-increasing energy demands, and devices based on perovskites and organic semiconductors offer further promise. Realizing a future of plentiful, low-cost renewable energy is within reach but requires improved characterization of next-generation PV materials. Today's AFMs provide a wide array of modes to visualize nanoscale structure and functional response, both in the dark and under variable illumination. Combined with higher spatial resolution, faster imaging, and greater environmental control, these benefits make AFMs indispensable for photovoltaics research.

Empower Your Photovoltaics Research with an Asylum AFM!

Email: AFM.info@oxinst.com, or
Call: +1-805-696-6466

References

1. A. Polman, M. Knight, E. C. Garnett, B. Ehrler, and W. C. Sinke, *Science* **352**, aad4424 (2016).
2. E. M. Tennyson, J. M. Howard, and M. S. Leite, *ACS Energy Lett.* **2**, 1825 (2017).
3. Y. Kutes, Y. Zhou, J. L. Bosse, J. Steffes, N. P. Padture, and B. D. Huey, *Nano Lett.* **16**, 3434 (2016).
4. J. Li, B. Huang, E. N. Esfahani, L. Wei, J. Yao, J. Zhao, and W. Chen, *npj Quantum Materials* **2**, 56 (2017).
5. N. D. Pham, V. T. Tiong, D. Yao, W. Martens, A. Guerrero, J. Bisquert, and H. Wang, *Nano Energy* **41**, 476 (2017).
6. Y. Shao, Y. Fang, T. Li, Q. Wang, Q. Dong, Y. Deng, Y. Yuan, H. Wei, M. Wang, A. Gruverman, J. Shield, and J. Huang, *Energy Environ. Sci.* **9**, 1752 (2016).
7. D. Moerman, G. E. Eperon, J. T. Precht, and D. S. Ginger, *Chem. Mater.* **29**, 5484 (2017).
8. I. M. Hermes, S. A. Bretschneider, V. W. Bergmann, D. Li, A. Klasen, J. Mars, W. Tremel, F. Laquai, H.-J. Butt, M. Mezger, R. Berger, B. J. Rodriguez, and S. A. L. Weber, *J. Phys. Chem. C* **120**, 5724 (2016).
9. J. Ciro, S. Mesa, J. I. Uribe, M. A. Mejia-Escobar, D. Ramirez, J. F. Montoya, R. Betancur, H.-S. Yoo, N.-G. Park, and F. Jaramillo, *Nanoscale* **9**, 9440 (2017).
10. J. R. O'Dea, L. M. Brown, N. Hoepker, J. A. Marohn, and S. Sadewasser, *MRS Bull.* **37**, 642 (2012).
11. M. Pfannmoeller, W. Kowalsky, and R. R. Schroeder, *Energy Environ. Sci.* **6**, 2871 (2013).
12. J. Yuan, M. J. Ford, Y. Zhang, H. Dong, Z. Li, Y. Li, T.-Q. Nguyen, G. Bazan, and W. Ma, *Chem. Mater.* **29**, 1758 (2017).
13. A. Gasperini, X. A. Jeanbourquin, and K. Sivula, *J. Polym. Sci., Part B: Polym. Phys.* **54**, 2245 (2016).
14. M. Kocun, A. Labuda, W. Meinhold, I. Revenko, and R. Proksch, *ACS Nano* **11**, 10097 (2017).
15. R. Giridharagopal, P. A. Cox, and D. S. Ginger, *Acc. Chem. Res.* **49**, 1769 (2016).
16. J. L. Garrett, E. M. Tennyson, M. Hu, J. Huang, J. N. Munday, and M. S. Leite, *Nano Lett.* **17**, 2554 (2017).
17. T.-H. Lai, S.-W. Tsang, J. R. Manders, S. Chen, and F. So, *Mater. Today* **16**, 424 (2013).
18. C. B. Jacobs, A. V. Ievlev, L. F. Collins, E. S. Muckley, P. C. Joshi, I. N. Ivanov, *J. Photonics Energy* **6**, 038001 (2016).

Acknowledgments

We thank R. Giridharagopal, B. Huey, and H. Phan for valuable discussions and L. Collins, R. Giridharagopal, D. Ginger, A. Gruverman, I. Hermes, B. Huey, J. Huang, I. Ivanov, F. Jaramillo, D. Moerman, N. Pham, Y. Shao, K. Sivula, V. Tiong, H. Wang, S. Weber, and J. Yuan for assistance with figure preparation.

Visit http://AFM.oxinst.com/PV to learn more

The foregoing brochure is copyrighted by Oxford Instruments Asylum Research, Inc. Oxford Instruments Asylum Research, Inc. does not intend the brochure or any part thereof to form part of any order or contract or regarded as a representation relating to the products or service concerned, but it may, with acknowledgement to Oxford Instruments Asylum Research, Inc., be used, applied or reproduced for any purpose. Oxford Instruments Asylum Research, Inc. reserves the right to alter, without notice the specification, design or conditions of supply of any product or service. Application Note 32 – 4/2018.

The Business of Science®

6310 Hollister Avenue
Santa Barbara, CA 93117
Voice +1 (805) 696-6466
Toll free +1 (888) 472-2795
Fax +1 (805) 696-6444

Web: http://AFM.oxinst.com
Email: AFM.info@oxinst.com